

Fabrication and Machinability of Mullite-ZrO₂-Al₂TiO₅ Ceramics

Young Been Shin, Won Jae Lee, and Il Soo Kim[†]

Department of Advanced Materials Engineering, Donggeui University, Busan 47340, Korea
(Received August 18, 2015; Revised August 27, 2015; Accepted August 27, 2015)

ABSTRACT

The machinability of materials is an important factor in engineering applications. Many ceramic components that have complex shapes require machining, typically using diamond tools, which leads to high production cost. Machinable ceramics containing h-BN have recently been developed, but these materials are very expensive because of high cost of raw materials and machining. Therefore the development of low-cost machinable ceramics is desirable. In this study, mullite-ZrO₂ ceramics were prepared additions of Al₂TiO₅, ZrSiO₄, Al₂O₃, and Al₂TiO₅ powders mixed at various molar ratios with sintering at 1400, 1500, and 1600°C for 1 hr. Phase formation and microstructure of the sintered ceramics were observed by XRD and SEM, respectively. The machinability of each specimen was tested using the micro-hole machining method. The machinability results show that the ceramics sintered at temperatures over 1500°C can be used as good low-cost machinable mullite-ZrO₂-Al₂TiO₅ ceramics.

Key words : Mullite-ZrO₂, Al₂TiO₅, Machinable ceramics, Reaction sintering

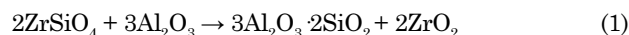
1. Introduction

Sintered ceramics normally have a high hardness, and they cannot be machined with common tungsten carbide tools. Thus ceramic components are often shaped and finished with diamond tools or by laser machining, whose cost sometimes exceeds more than half of the production cost.¹⁾ Ceramic parts are inherently strong, abrasion resistant, and chemically stable. Furthermore, they have high refractoriness, electrically insulating property, and excellent dielectricity. If, in addition, they are easily machinable, their application can be extended much further. For a given material, its strength (or hardness) and machinability are, however, contradicting each other, and it is very difficult to have a strong and machinable material.

Various ceramics have been incorporated with layered-structure additives to give a certain degree of machinability: For example, mica-added systems²⁻⁴⁾ have been used for long time, and h-BN-added systems⁵⁻¹¹⁾ have been extensively studied recently. Thus, it is possible to machine these materials with high-speed steel or tungsten carbide tools owing to the cleaving property of additives. However, mica-added systems are normally inferior in properties, and h-BN as raw material is very expensive. The h-BN-added ceramics also require high sintering cost. Addition of aluminium titanate (Al₂TiO₅), although its crystal structure is different from the two additives mentioned above, exhibits similar fracture mode and provides corresponding effects.¹²⁻¹⁴⁾

Mullite is a superior ceramic material with an excellent

chemical stability, high-temperature strength, and thermal shock resistance. Especially, mullite synthesized by the following reaction can achieve reaction and sintering simultaneously, and strengthening effect by ZrO₂ phase transformation can be expected.



In this study, by adding Al₂TiO₅ into the reactants of the above reaction, we prepared three-phase ceramics consisted of mainly mullite, ZrO₂, and Al₂TiO₅. And we evaluated their machinability in terms of the ratio of three reactants, phase contents in the sintered body, and sintered microstructures. Based on the results, we provided the optimum condition for the preparation of machinable ceramics.

2. Experimental Procedure

Raw materials used for this study are: ZrSiO₄ (99.9%, 1 μm, Junsei Chemical), α-Al₂O₃ (99.9%, 1 μm, AES-11, High Purity Chemicals), and Al₂TiO₅ (99.9%, 1 μm, Sigma-Aldrich). Their mixing ratios are so adjusted that the mullite/Al₂TiO₅ mole ratio after reaction sintering become 1/1, 1/1.5, and 1/2. The powder mixture was milled with acetone in a planetary mill (pulverisette 5, FRITSCH) with milling balls consisted of 5 mm Al₂O₃ and 5 and 2 mm ZrO₂ in a ratio of 1 : 1 : 2, respectively. The vol.% of charged powder, solvent, and milling media was 10 : 40 : 50, and milling was carried out at 300 rpm for 24 h. The milled slurry was filtered through filter paper on a plaster board, and dried in a dryer at 60°C for 24 h.

The dried powder was broken in a mortar, and formed with the addition of 5% PVA (polyvinyl alcohol) as a binder under uniaxial pressure of 1 ton/cm² for 30 sec. The preformed samples were further cold-isostatically pressed at

[†]Corresponding author : Il Soo Kim

E-mail : iskim@deu.ac.kr

Tel : +82-51-890-1715 Fax : +82-51-890-2631

250 MPa for 10 min. We sintered the formed samples at 1400, 1500, and 1600°C for 1 h in air by using a heating rate of 5°C/min.

We measured densities of the sintered samples, and analysed their phases by XRD (PANalytical X'Pert PRO MPD). We also evaluated their microstructural developments by FE-SEM (Quanta2000FEG, FEI company). We determined the machinability by drilling a hole in each sample with carbide drill bits (dia. 0.6 mm) at 3,000 rpm in 5 steps. We used a micro-drilling machine (MM-250S3, MANIX CNC), and kept the hole-to-hole distance wider than 1 mm. The loads (Newton) against drilling for each specimen generated during drilling were measured for 30 seconds by a force calibration apparatus (Sensor 9345B, Charge Meter 5015A, KISTLER AG) attached to the machine. We observed the conditions of drilled holes by optical microscope and SEM.

3. Results and Discussion

Figure 1 shows XRD results of samples sintered at each temperature in terms of the mullite/ Al_2TiO_5 mol ratio (M/AT ratio from now on). Here, intensities are normalized to the same strength to compare relative crystallinity, which are 1/2, 1/1.5, and 1/1, respectively from the top. Note that ZrO_2 is as monoclinic phase.

Tetragonal ZrO_2 can transform to monoclinic phase by mechanical impact during powder preparation for XRD analysis. It is reported that phase transformation can even occur by mechanical stress during ball milling of raw material in powder form.¹⁵⁾ And it also can happen by microcrack propagation of Al_2TiO_5 during sample cooling, and by subsequent energy absorption that leads to phase transformation to monoclinic phase.¹³⁾ Since this topic of ZrO_2 strengthening effect is out of the scope of this study, we did not attempt to identify the phase fraction of the two phases.

At 1400°C, the intended reaction sintering seems to be not complete, and a considerable amount of unreacted ZrSiO_4 and Al_2O_3 phases are left over, while the peaks of products, mullite and m- ZrO_2 , are still low. At temperatures higher than 1500°C, however, there is no unreacted phase, and only ZrO_2 , mullite, and AT(Al_2TiO_5) peaks show up. With α - Al_2O_3 as raw material, reaction via Eq. (1) is thermodynamically possible above 1447°C. In practice, however, it is not easy to achieve both complete reaction and densification simultaneously even above this temperature due to slow solid-state diffusion. Reaction sintering under no applied pressure can only be conveniently achieved via two-step sintering, or with sintering additives such as TiO_2 , MgO , CaO , and CeO_2 .¹⁶⁻¹⁸⁾

Figure 2 is a schematic of reaction and growth of ZrO_2 nuclei at the amorphous mullite phase in the matrix. At the initial stage of reaction, ZrO_2 grains grow in a spherical shape by bulk diffusion in the amorphous mullite. As mullite phase gradually becomes crystalline, $\text{Al}_2\text{O}_3/\text{SiO}_2$ ratio changes, and diffusion becomes slower accordingly, and

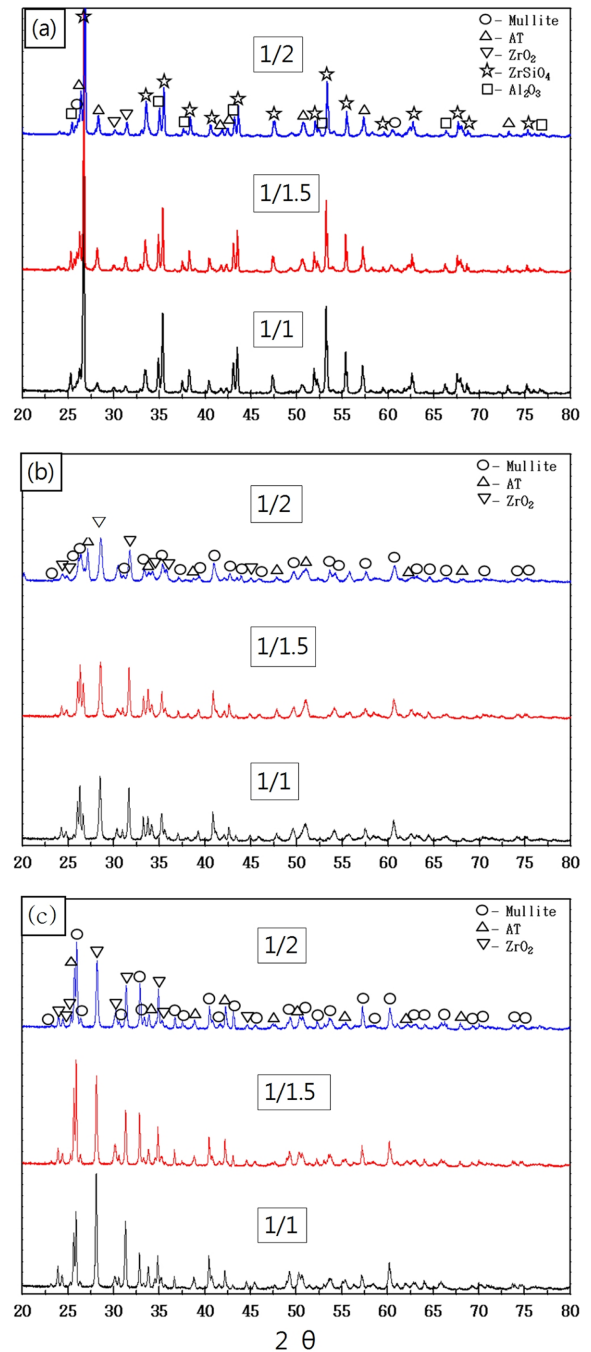


Fig. 1. XRD patterns of specimens with various mol ratios of mullite/ Al_2TiO_5 (M/AT) sintered at (a) 1400°C (b) 1500°C (c) 1600°C.

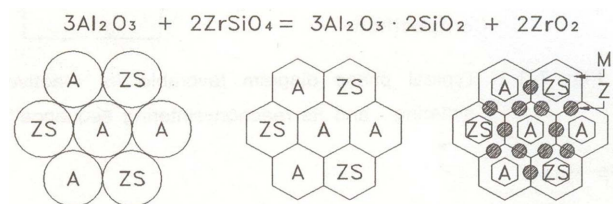


Fig. 2. Schematic of microstructural development by reaction sintering of α - Al_2O_3 and ZrSiO_4 .¹⁹⁾

ZrO₂ grains grow via grain-boundary diffusion.²⁰⁾

XRD results indicate that the reaction starts to proceed at 1400°C, which is lower than the theoretical reaction temperature. We assume that the added Al₂TiO₅ enhances the reaction like other reported studies with sintering additives. The argument is supported by the lowered ZrSiO₄ peak and the increased ZrO₂ peak at 1400°C as Al₂TiO₅ ratio is increased.

At 1500 and 1600°C, reaction sintering completely consumed reactants, and only peaks from ZrO₂, mullite, and Al₂TiO₅ show up. At 1500°C, peaks of product phases are low but Al₂TiO₅ peak is considerable. At 1600°C, peak intensities of mullite and ZrO₂ increased compared to those of 1500°C, which is indicative of increasing crystallinity at elevated temperatures. In view of the M/AT ratio, as the amount of mullite increases, ZrO₂ peak goes upward, while the relatively peak of Al₂TiO₅ goes downward.

Table 1 shows densities of each sample. For sample sintered at 1400°C, its density decreases with increasing the M/AT ratio. However, for the cases of 1500°C and 1600°C, increasing the M/AT ratio increases density. As shown in Fig. 1(a), although reaction sintering at 1400°C is insignificant, increasing the M/AT ratio results in lowering unreacted ZrSiO₄ phase. Theoretical densities of the involved phases are: ZrSiO₄; 4.56 g/cm³, Al₂O₃; 3.99 g/cm³, mullite; 3.16 g/cm³, m-ZrO₂; 5.68 g/cm³, and Al₂TiO₅; 3.40 g/cm³. Since all five phases are co-present in the sample fired at 1400°C, it is difficult to estimate the density variation. We, however, assumed that sample density decreases with increasing the M/AT ratio due to less presence of ZrSiO₄ of high theoretical density in the microstructure.

Samples sintered at 1500 and 1600°C show no unreacted phase, and their densities increase with increasing AT fraction, since Al₂TiO₅ has higher density than that of mullite. Sample sintered at 1500°C results in a relatively high density compared to that of 1600°C, probably due to relatively less reaction and amount of product phase. Fig. 3 is SEM image (X1,000) of sample sintered at 1500°C (M/AT = 1/1), that shows no particular difference from microstructures of other samples. They all show small particles of products in the growing process, distributed on plat grains as already indicated by XRD data above.

Figure 4 compares two microstructures (X3,000) of 1/1 and 1/2 samples. The 1/1 sample shows only trace of needle-shape grains. The 1/2 sample shows a better densification and more grain growth. The same trend appears in the sintered sample at 1600°C. Fig. 5 is microstructural images (X1,000) of 1/1 and 1/2 samples. Compared to 1/1 sample, 1/2 sample has fewer pores and well-defined larger grains in a

Table 1. Densities (g/cm³) of Each Specimens

Sintering temp.	M/AT mol ratio 1/1	1/1.5	1/2
1400°C	4.50	4.33	4.30
1500°C	3.80	3.82	3.91
1600°C	3.52	3.63	3.70

uniform distribution. As mentioned above, this attributes to the action of Al₂TiO₅ as a sintering aid. Increasing density with an increase in the M/AT ratio also contributes to a denser microstructure.

Figure 5(b) and its magnified version (Fig. 6) show a morphology of co-existing isotropic and columnar grains. Cracks can be observed in various parts of microstructure including a crack across a whole grain. More cracks are observed with the increasing M/AT ratio. Fig. 7 is EDS analysis of grain with crack (A) and of isotropic grain (B). Grain A reveals O, Al, and Ti peaks, suggesting that it is Al₂TiO₅. Al₂TiO₅ is known to be very anisotropic as a single crystal, while to be a low expansion material by compensating anisotropy as a polycrystal. Normally, grain anisotropy generates many micro-cracks during the cooling process after sintering,²¹⁾

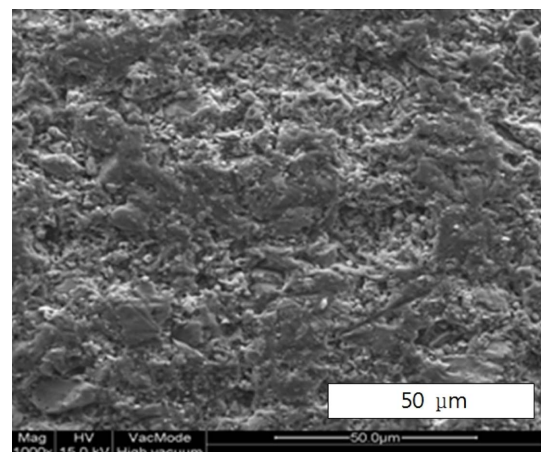


Fig. 3. SEM image of specimen sintered at 1500°C with M/AT mol ratio of 1 / 1.

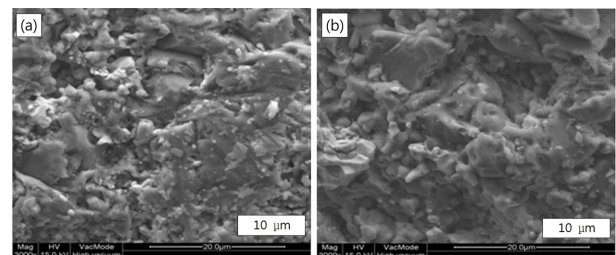


Fig. 4. Comparison of SEM image of specimens sintered at 1500°C with different M/AT mol ratio of (a) 1 / 1 and (b) 1 / 2.

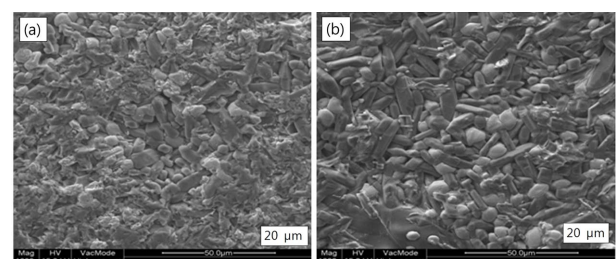


Fig. 5. Comparison of SEM image of specimens sintered at 1600°C with different M / AT mol ratio of (a) 1 / 1 and (b) 1 / 2.

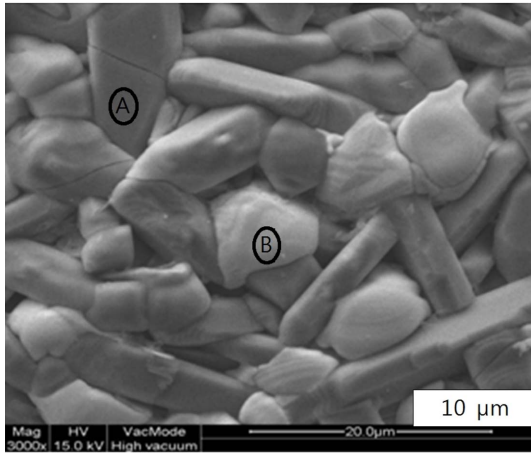


Fig. 6. Magnified ($\times 3$) image of the Fig. 5(b).

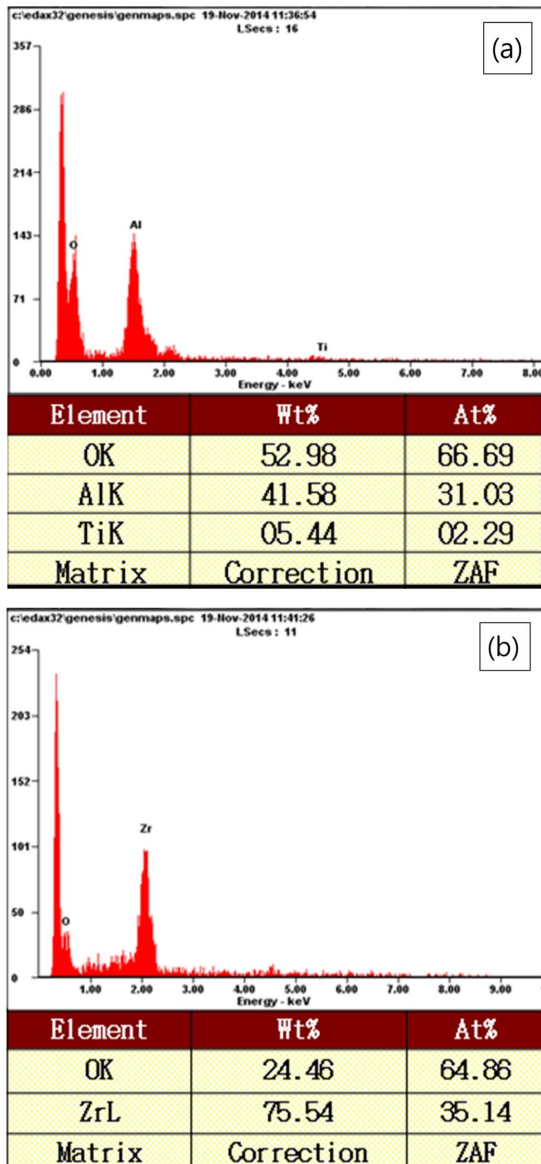


Fig. 7. EDX analyses for the round field of Fig. 6 (a) A and (b) B.

and causes a decrease in strength. On the other hand, however, micro-crack can absorb strain energy and impede crack propagation, which leads to an enhanced thermal shock resistance.²²⁾ This mechanism can act positively on machinability, since crack propagation of the inherent brittle ceramics can be obstructed at micro-cracks, and shear wave can be diminished and absorbed at micro-cracks during machining.

Grain B represents ZrO_2 grain since EDS results show only O and Zr peaks. ZrO_2 grains are appeared relatively bright in the image. Mullite grain is typically in a needle shape, and it is safely assumed that columnar grains without crack are mullite. A comparative study on a Al_2TiO_5 added Al_2O_3 and a reaction sintered $Al_2O_3-TiO_2$ reported that needle-like mullite crystals were found in the microstructure.¹²⁾ Calculated volume ratios of each phase in sample 1/1 and 1/2 are; mullite: Al_2TiO_5 : ZrO_2 = 58:23:18 and 48 : 37 : 15, respectively.

Table 2 is a summary of drilling test showing mean values of the load (Newton) against drilling for each specimen measured by a force calibration apparatus attached to CNC micro-milling machine. As sintering temperature decreases or the amount of Al_2TiO_5 increases, machining becomes easier, if we neglect the partially-sintered sample at 1400°C. Samples sintered at 1600°C with 1/1 and 1/1.5 ratios are also not considered here, since the machining has damaged drill tips so severely that machining became impossible. Machining of the 1/2 sample is relatively smooth, although machining resistance is relatively high compared to other samples.

Figure 8 is images of drilled holes for two samples by an optical microscope, which indicates a very clean drilling. Metals are normally machined by the formation of shear

Table 2. Mean Value of the Load (N) against Drilling for Each Specimens

Sintering temp.	M/AT mol ratio 1/1	1/1.5	1/2
1400°C	4.81	3.50	3.24
1500°C	11.68	8.23	6.64
1600°C	-	-	31.50

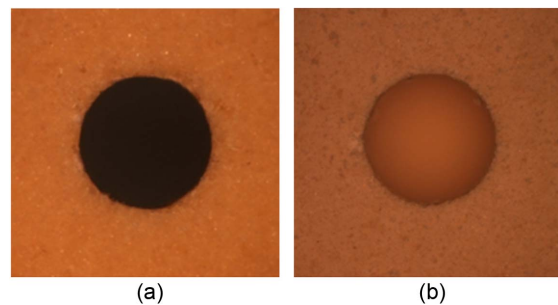


Fig. 8. OM images of (M/AT = 1 / 2) specimens sintered at different temperatures after micro drilling (a) 1500°C (b) 1600°C.

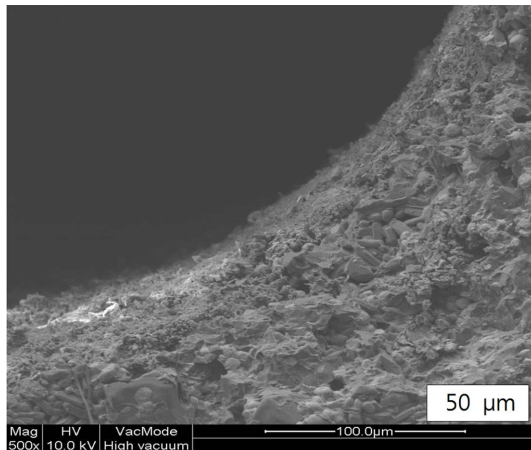


Fig. 9. SEM image of specimen (M/AT = 1/2) sintered at 1600°C after micro drilling.

fracture planes in the plastic deformation zone ahead of the moving tool. Both shear and compressive stresses developed in the zone lead to cutting. On the contrary, ceramics with free cutting ability are machined by shear wave ahead of cutting tool followed by a series of inter- and intra-granular fractures. To make this mechanism operative, presence of micro-cracks or cleavage plane in the microstructure is required to impede crack propagation, to absorb stress, and to proceed cutting.¹⁾

Figure 9 is SEM image of the sample of Fig. 8(b), showing deep and clean material-removal without generating any crack around the drilled hole by machining load. It seems that crack propagation by machining is constrained by micro-cracks on Al₂TiO₅ grains, and mullite and ZrO₂ grains with higher strength and hardness than those of Al₂TiO₅ effectively make up the necessary mechanical properties. The included ZrO₂ grains further provide crack bridging to block crack advance.¹³⁾

4. Conclusions

We prepared free cutting ability ceramics of mainly three phases by reaction sintering of ZrSiO₄ and Al₂O₃ to form mullite (3Al₂O₃·2SiO₂)-ZrO₂ composite, and by adding Al₂TiO₅ in proper ratios as the third phase. Added amounts of Al₂TiO₅/mullite were 1/1, 1/1.5, and 1/2 mole ratio, and their sintering were carried out at 1400, 1500, and 1600°C for 1 h. XRD results showed only peaks of mullite, ZrO₂, Al₂TiO₅ without any peak of ZrSiO₄ and Al₂O₃ at temperatures above 1500°C. Increase in the amount of Al₂TiO₅ greatly enhanced their reaction and sintering. We conclude from the results of machinability assessments by the micro-hole machining method that micro-cracks present in Al₂TiO₅ grains improve machinability by impeding crack propagation and adsorbing stresses. All samples sintered at 1500°C were machined easily, and those samples sintered at 1600°C were machined easily only when the mullite/Al₂TiO₅ mole ratio was 1/2.

Acknowledgments

This study is supported by Intra-fund 2015 of Donggeui University.

REFERENCES

1. P. Blake, T. Bifano, T. Dow, and R. O. Scattergood, "Precision Machining of Ceramic Materials," *Ceram. Bull.*, **67** [6] 1038-43 (1988).
2. C. K. Chyung, G. H. Beall, and D. G. Grossman, "Microstructure and Mechanical Properties of Mica Glass-Ceramics," pp. 1167-94 in 10th Int. Congress on Glass. Ed. by M. Kunugi, Kyoto, 1974.
3. S. Taruta, R. Fujisawa, and K. Kitajima, "Preparation and Mechanical Properties of Machinable Alumina/Mica Composites," *J. Eur. Ceram. Soc.*, **26** 1687-93 (2006).
4. B. Ashouri Rad and P. Alizadeh, "Pressureless Sintering and Mechanical Properties of SiO₂-Al₂O₃-MgO-K₂O-TiO₂-F (CaO-Na₂O) Machinable Glass-Ceramics," *Ceram. Int.*, **35** 2775-80 (2009).
5. Y. Li, G. Quio, and Z. Jin, "Machinable Al₂O₃-BN Composite Ceramics with Strong Mechanical Properties," *Mater. Res. Bull.*, **37** 1401-9 (2002).
6. Y. S. Yoon, J. H. Lee, W. S. Cho, M. W. Cho, and E. S. Lee, "Mechanical Properties and Machinability of Machinable Ceramics (in Korean)," *Ceramist*, **6** [3] 12-7 (2003).
7. B. Zhong, G. L. Zhao, X. X. Huang, L. Xia, X. H. Tang, S. C. Zhang, and G. W. Wen, "Microstructure and Mechanical properties of ZTA/BN Machinable Ceramics Fabricated by Reactive Hot Pressing," *J. Eur. Ceram. Soc.*, **35** 641-49 (2015).
8. S. Y. Beck, M. W. Cho, and W. S. Cho, "Mechanical Properties and End-Milling Characteristics of AlN-hBN Based Machinable Ceramics," *J. Korean Ceram. Soc.*, **45** [1] 75-81 (2008).
9. H. Wu and W. Zhang, "Fabrication and Properties of ZrB₂-SiC-BN Machinable Ceramics," *J. Eur. Ceram. Soc.*, **30** 1035-42 (2010).
10. H. Y. Jin, W. Wang, J. Q. Gao, G. J. Qiao, and Z. H. Jin, "Study of Machinable AlN/BN Ceramic Composites," *Mater. Lett.*, **60** 190-93 (2006).
11. A. Kovalcicova, J. Balko, C. Balazsi, P. Hvizdos, and J. Dusza, "Influence of h-BN Content on Mechanical and Tribological Properties of Si₃N₄/h-BN Ceramic Composites," *J. Eur. Ceram. Soc.*, **34** 3319-28 (2014).
12. J. H. Park, W. J. Lee, and I. S. Kim, "Al₂TiO₅-Machinable Ceramics Made by Reactive Sintering of Al₂O₃ and TiO₂," *J. Korean Ceram. Soc.*, **47** [6] 498-502 (2010).
13. J. H. Park, D. S. Jung, W. J. Lee, and I. S. Kim, "Machinable Ceramics Made by the Reactive Sintering of PSZ, Al₂O₃ and TiO₂," *J. Korean Ceram. Soc.*, **49** [6] 581-85 (2012).
14. I. S. Kim, J. H. Park, W. J. Lee, and K. H. Lee, "Machinable SiC Ceramics with Addition of Al₂TiO₅," *J. Korean Ceram. Soc.*, **50** [6] 372-77 (2013).
15. T. Shimada, M. Mizuno, K. Katou, Y. Nurishi, M. Hashiba, O. Sakurada, D. Mizuno, and T. Ono, "Aluminium Titanate - Tetragonal Zirconia Composite with Low Thermal Expan-

- sion and High Strength Simultaneously," *Solid State Ionics*, **101-10** 1127-33 (1997).
16. N. Claussen and J. W. Jahn, "Mechanical Properties of Sintered, in situ Reacted Mullite-zirconia Composites," *J. Am. Ceram. Soc.*, **63** [3-4] 228-29 (1980).
 17. P. Descamps, "High Temperature Characterization of Reaction Sintered Mullite-zirconia Composites," *J. Am. Ceram. Soc.*, **74** 2476-81 (1991).
 18. I. S. Kim and H. W. Hennicke, "Mullit-ZrO₂-Keramik mit Zusätzen von Bentonit, Speckstein und MnO+TiO₂," *Keram. Z.*, **43** 466-68 (1991).
 19. J. G. Lee, "Sintering of Ceramics," pp. 146, Bando Press, Seoul, 1994.
 20. J. S. Wallace, "Microstructure and Property Development of in situ Reacted Mullite-ZrO₂ Composites," *Adv. Ceram. Soc.*, **12** 436-42 (1984).
 21. H. A. J. Thomas and R. Stevens, "Aluminium Titanate - A Literature Review," *Br. Ceram Trans. J.*, **88** 144-51 (1989).
 22. I. J. Kim and C. Zografou, "Thermal Shock Resistance of Al₂TiO₅ Ceramics Prepared from Electrofused Powders," *J. Korean Ceram. Soc.*, **35** [10] 1061-69 (1998).